

Experiments on a magnetically levitated planar actuator

No. 69

C.M.M. van Lierop, J.W. Jansen, E.A. Lomonova & P.P.J. van den Bosch

Eindhoven University of Technology, Department of Electrical Engineering, P.O. Box 513, 5600 MB Eindhoven, the Netherlands, C.M.M.v.Lierop@tue.nl, J.W.Jansen@tue.nl

ABSTRACT: This paper discusses experimental results of a moving-magnet planar actuator with integrated magnetic bearing called the Herringbone Pattern Planar Actuator (HPPA). Both open-loop measurements of the commutated planar actuator as well as measurements of the closed-loop dynamic performance of the operational actuator are included. Smooth switching between different sets of active coils is used to enable long stroke motion in the xy -plane using a special commutation algorithm. The constraints imposed by the current amplifiers in combination with the commutation algorithm result in complex, position dependent, worst-case acceleration constraints. Therefore, a novel method is presented to derive the worst-case acceleration specification in the xy -plane, as a function of position and current amplifier constraints.

1 INTRODUCTION

Magnetically levitated planar actuators are developed as alternatives to xy -drives constructed of stacked linear motors. Although the translator of these ironless planar actuators can move over relatively large distances in the xy -plane only, it has to be controlled in six degrees-of-freedom (DOF) because of the active magnetic bearing. The advantage of magnetically levitated planar actuators is that they can operate in vacuum, for example in extreme-UV lithography equipment. Planar actuators can be constructed in two ways. The actuator has either moving coils and stationary magnets or moving magnets and stationary coils (Jansen, J.W. et al. 2007a). The last type of planar actuator does not require a cable to the moving part. However, only the coils underneath the translator can significantly contribute to its levitation and propulsion. Therefore, the set of active coils needs to change with the position of the translator during movements in the xy -plane. A special commutation strategy called direct wrench-current decoupling has been derived which allows for switching between different active sets of coils without influencing the decoupling of the force and torque components (Lierop, C.M.M. van et al. 2006, Lierop, C.M.M. van et al. 2007). Due to the switching and the need to decouple both the force and

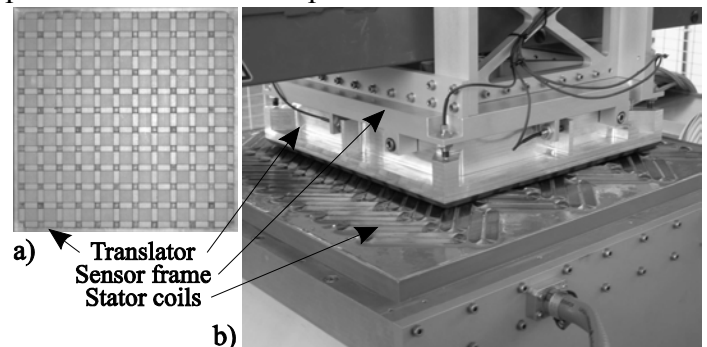


Figure 1. a) Magnet array (bottom view). b) Overview of the planar actuator with sensor frame.

the torque, the resulting current waveforms are non-sinusoidal and each stator coil needs to be controlled individually using a single phase amplifier. A prototype moving-magnet planar actuator has been built (Figure 1) called the Herringbone Pattern Planar Actuator (HPPA) after its stator coil layout (Jansen, J.W. et al. 2007a).

In this paper the result of several experiments are discussed. However, due to the non-sinusoidal current waveforms and the individually excited coils, finding the worst-case acceleration specifications is not straightforward. Therefore, first a method is discussed in this paper which can be used to find the worst-case acceleration specification as a function of the current amplifier constraints and the position in the xy -plane, to assure valid input force and torque combinations and correct input trajectories which do

not exceed the current constraints of the power amplifier during the experiments.

In section 4 of this paper two types of measurements performed on the HPPA are discussed. Firstly, open-loop commutated force and torque measurements have been performed in order to validate the (static) decoupling of the force and torque components using the special commutation strategy. Secondly, the dynamical closed-loop system is discussed and the structured error dynamics are derived and measured. The structured error dynamics of the planar actuator lead to specifications related to the implementation of the commutation strategy. Moreover, the closed-loop performance is measured using a demanding trajectory. The resulting tracking errors are discussed in this paper.

2 HPPA TOPOLOGY

Figure 1 shows a photo of the HPPA planar actuator and a bottom view of the magnet array. The translator consists of a permanent magnet array with a quasi-Halbach magnetization. The stator of the actuator consists of 84 coils in a herringbone pattern of which only 24 are simultaneously energized. A schematic drawing of the actuator is shown in Figure 2. The properties and dimensions of the actuator are summarized in Table 1.

Table 1. properties and dimensions of the HPPA.

Size Translator	300 × 300 mm
Mass Translator M	8.2 kg
Mechanical clearance (z-dir)	1 - 2 mm
Speed (xy-plane)	1.0 m/s
Acceleration (xy-plane)	10 m/s ²
Pole pitch τ	25 mm

Because the shape of the rectangular coil is optimized, the force production in the xy -plane is physically decoupled (Jansen, J.W. et al. 2007b). This reduces cross-talk between the degrees-of-freedom and, therefore, simplifies the modeling of the force and the torque in the actuator. When applying the $dq0$ decomposition, the quadrature and direct component represent the drive and lifting force, respectively. However, when using this decomposition, the distribution of the forces over the surface of the translator is ignored resulting in an uncontrolled disturbance torque (Lierop, C.M.M. van et al. 2007). Therefore, in planar actuators in which both the force and the torque are controlled using the same set of coils, a different inverse transformation called the direct wrench-current decoupling should be applied (Lierop, C.M.M. van et al. 2006). The planar

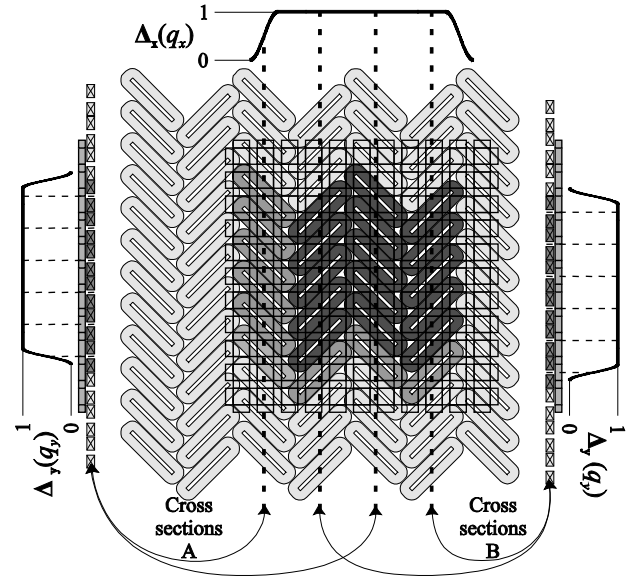


Figure 2. Schematic topview (using a transparent magnet-array) of the HPPA topology with the two smooth weighting functions Δ_x and Δ_y .

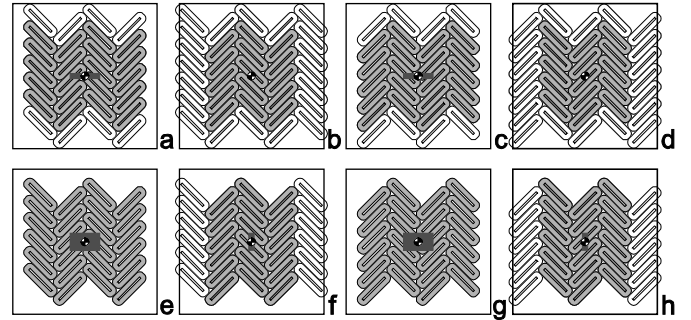


Figure 3. Two basic coil layouts (e and g) and the six corresponding switching boundaries (a, b, c, d, f, and h) to obtain long stroke planar motion where the grey coils are active and the white coils inactive.

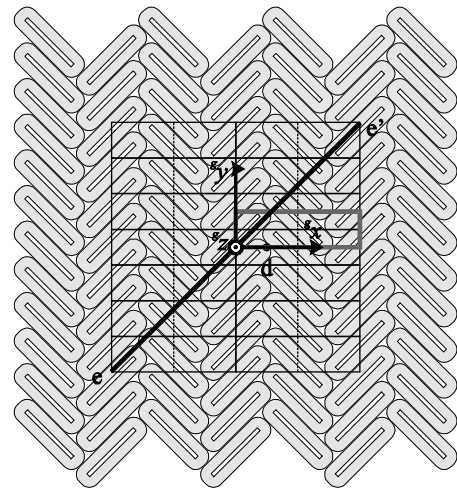


Figure 4. The positions of the mass center point of the translator of the HPPA at which switching to different coil sets occurs (fig. 3) are indicated by the black rectangles. The grey rectangle shows the xy measurement range of the open-loop experiments. The point d is the position at which the frequency response measurements of figure 15 have been performed. The diagonal black line shows the measurement trajectory e-e' of the closed loop experiment shown in figure 16.

actuators considered can be described by the following mapping (Jansen, J.W. et al. 2007b)

$$\mathbf{w} = \mathbf{\Gamma}(\mathbf{q}) \mathbf{i} \quad (1)$$

assuming that they have a linear relation between the current vector \mathbf{i} [A] and the wrench vector \mathbf{w} [N], [Nm] (consisting of the force and torque components) described by the matrix $\mathbf{\Gamma}$ [N/A],[Nm/A] of which the elements are a non-linear function of the position and orientation vector \mathbf{q} [m], [rad]. There are more constraints needed to arrive at a unique solution to the inverse transformation because there are more active coils than DOF. A possible solution can be obtained by minimizing the ohmic losses in the coils. To obtain a fast real-time implementation only the coils that are underneath the magnet-array are considered, which reduces the dimensions of the current vector \mathbf{i} and, consequently, the matrix $\mathbf{\Gamma}$ and allows for model simplification by ignoring the edge effects of the magnet-array. However, this introduces the need for an additional constraint which allows for smooth switching between active coil sets. This is done by adding smooth position dependent weighting functions $\Delta(\mathbf{q}) = \Delta_x(\mathbf{q}) \Delta_y(\mathbf{q})$ which are shown in Figure 2. The weighting functions smoothly penalize the active coils which leave the surface of the magnet array without influencing the decoupling, resulting in the following solution to the inverse problem (Lierop, C.M.M. van et al. 2006)

$$\mathbf{i}_{des} = \mathbf{q} \mathbf{w}_{des}^{-1} \Delta(\mathbf{q}) \mathbf{\Gamma}^{-1}(\mathbf{q}) \mathbf{w}_{des} \quad (2)$$

The HPPA topology has two basic active stator coil layouts which consist of 24 coils. To switch between these layouts there are six different switching boundary situations in which there are less active coils. The two basic coil layouts and the six switching boundary situations are shown in Figure 3. Figures 3e and 3g show the two basic coil layouts with their admissible sets of xy positions (indicated by the grey rectangles) for the mass center point of the magnet array. To switch between both basic coil layouts six switching topologies are necessary which have less active coils (indicated by the grey coils of Figures 3a-3d, 3f and 3h). The admissible sets of xy positions for the mass center point of the magnet array corresponding to the six switching topologies are shown by the grey lines in figures 3a, 3c, 3f and 3h and by the points in figures 3b and 3d, respectively. When the inverse transformation given by (2) is non-singular over all admissible xy positions for all necessary active coil topologies indicated in Figure 3 the stator coil pattern can then be repeated infinitely in the xy -plane without losing

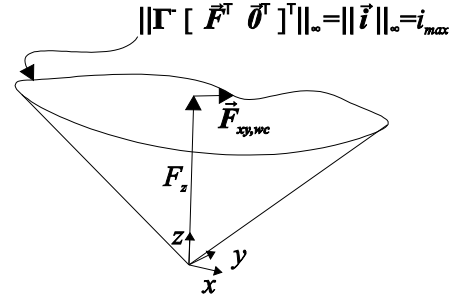


Figure 5. Illustration which indicates how the worst-case (smallest) acceleration vector (where one or more of the stator coil currents will clip) can be found at a given position and orientation \mathbf{q} when using the direct wrench-current decoupling $\mathbf{\Gamma}^{-1}(\mathbf{q})$.

controllability of the actuator. Consequently, the planar topology can, in principle, have an infinite stroke in the xy -plane.

3 WORST-CASE FORCE COMPONENTS

Traditionally, the $dq0$ transformation is used which results in relatively simple bounds on the maximum force or acceleration. However, due to the non-sinusoidal waveforms and the switching of active coil sets, the calculation of the maximum acceleration as a function of the current constraints of the amplifier demands for a highly non-convex minimization problem. Due to the constant levitation force and the non-linear decoupling it is not straightforward to find the maximum acceleration specifications due to current amplifier constraints. This section focuses on the worst-case (smallest) acceleration specification of the HPPA which can be achieved in the xy -plane when using the direct wrench-current decoupling and switching between active coils (section 2).

When the actuator is considered to have a perfect magnetic bearing, meaning no angle variation and, therefore, zero torque, a maximum amplifier current for each amplifier i_{max} of 6 A and a worst-case maximum constant clearance of $q_z = 2$ mm, it is possible to determine the large signal bounds on the force in the xy -plane $\mathbf{F}_{xy} = [F_x \ F_y]^T$ by the following minimization problem

$$\mathbf{F}_{xy,wc} = \arg \min_{\mathbf{F}_{xy}} \|\mathbf{F}_{xy}\|_2 \quad (3)$$

$$\mathbf{w} = \begin{bmatrix} \mathbf{F}_{xy}^T & F_z & \mathbf{T}^T \end{bmatrix}^T$$

$$\mathbf{T} = 0, \quad F_z = Mg$$

$$\|\mathbf{i}\|_{\infty} = i_{max}$$

The (highly non-convex) minimization searches for the worstcase (minimal) amplitude of the force vector in the xy -plane (using the direct wrench-current decoupling) for which the infinity norm of the current

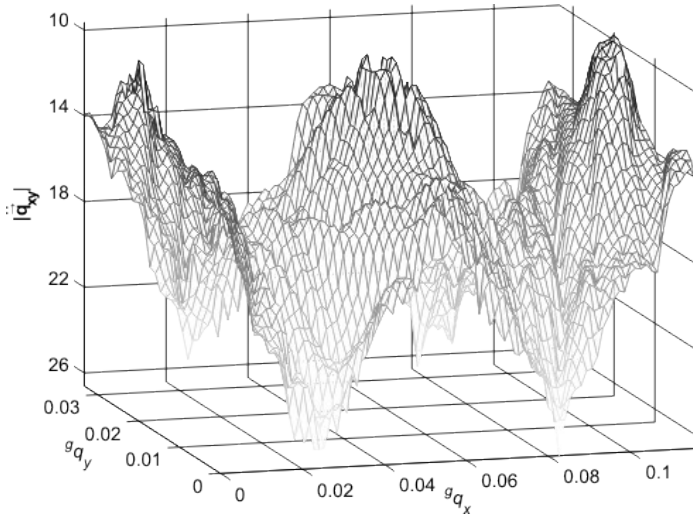


Figure 6. Worst-case amplitude of the acceleration vector in the xy -plane $\|\mathbf{q}_{xy}\|_2$ m/s² at a clearance of 2 mm.

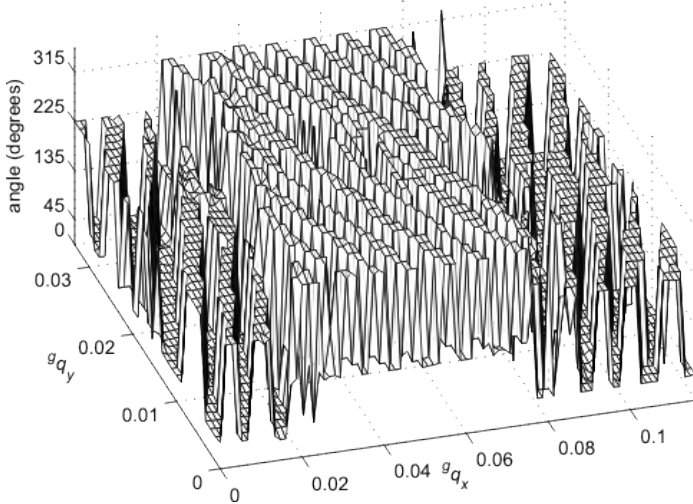


Figure 7. Worst-case direction of the acceleration vector in the xy -plane. The direction is specified by the angle of the vector \mathbf{q}_{xy} with respect to the x axis at a clearance of 2mm.

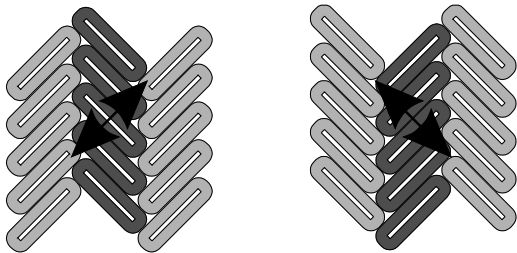


Figure 8. The two active coil topologies corresponding to the directions of the worstcase acceleration vector in the xy -plane. Where only the dark-gray coils can be used for the acceleration in the worst-case direction.

vector equals the maximum current i_{max} (meaning that one or more of the coil currents will clip against the current amplifier constraints), while maintaining a constant levitation force in the z -direction $F_z = Mg$ (where M is the total mass of the translator and g is the gravitational constant). The resulting force vector

$\mathbf{F}_{xy,wc}$ is the worst case (smallest) acceleration force in the xy -plane at a given position, illustrated by figure 5. The worst case acceleration in the xy -plane \mathbf{q}_{xy} can be derived from the worst case forces by dividing them by the total mass of the translator (ignoring the damping, $D < 1$ Ns/m at 2 mm clearance, of the system). The amplitude of the worst case acceleration and the angle of the vector in the xy -plane with respect to the x axis are shown for the HPPA topology in Figures 6 and 7 respectively, using a mass of 8.2 kg and an air-gap (clearance) of 2 mm. From these pictures it can be seen that it is possible to obtain an acceleration of at least 10 m/s² in all directions of the xy -plane. The smallest worst case acceleration and its direction can be explained by looking at the worst case switching topologies of the HPPA shown in Figure 8. The darker columns of stator coils shown in Figure 8 are the only coils which can generate a force in the smallest worst case acceleration direction. Therefore, since the amount of coils which can generate a force in the worst case direction is smallest it is obvious that the current through one of these coils will be the highest.

4 EXPERIMENTS

An experimental setup has been built in order to validate the electromechanical design and the derived control strategy. The measurements on the HPPA are carried out on a test bench, which is constructed on top of an Assembléon H-drive. This gantry consists of three linear motors. Two motors are positioned in parallel (the y_1 - and y_2 -motors). Between the translators of these motors a third linear motor is mounted (the x -motor) which enables planar motion of its translator. By displacing the parallel y_1 - and y_2 -motors with respect to each other, the x -motor can rotate about the z -axis (5 mrad). Figure 13 shows an overview of the test-bench and its control hardware. A dSPACE DS1005MP modular DSP system is used with two processor boards. One board is used for IO interfacing and H-drive (and HPPA) safety and control, while the other processor board is used for the real-time commutation of the HPPA prototype. The IO-interface which provides the setpoints to the 84 amplifier channels of the prototype are consists of 28 RS485 serial interfaces. The sample frequency is set to 4kHz.

4.1 Open-loop experiments

The translator of the HPPA can be mounted via a 6-DOF load cell (JR3 45E15A4-I63-S 100N10) to the translator of the x -motor of the H-drive. The H-drive

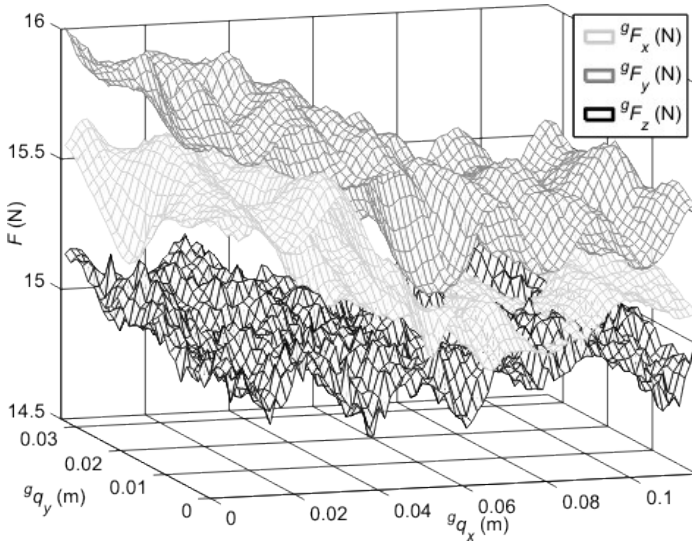


Figure 9. Measured force components sF_x , sF_y and sF_z of the open-loop commutated HPPA, using a desired wrench vector ${}^s\mathbf{w}_{\text{des}} = [15 \ 15 \ 15 \ 0 \ 0 \ 0]^T$ and a clearance of 1.5 mm

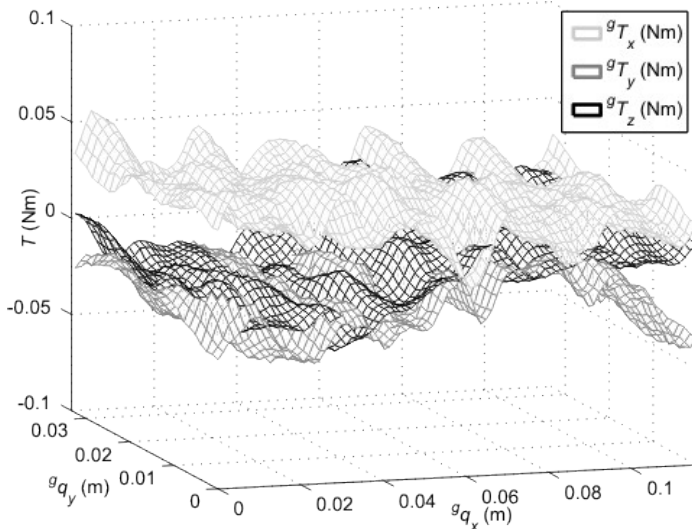


Figure 10. Measured torque components sT_x , sT_y and sT_z of the open-loop commutated HPPA, using a desired wrench vector ${}^s\mathbf{w}_{\text{des}} = [15 \ 15 \ 15 \ 0 \ 0 \ 0]^T$ and a clearance of 1.5 mm

can be used to position the translator of the HPPA above its stator coils. Using this configuration of the test bench, the open-loop response of one xy area of repetition indicated by the grey rectangle in figure 4 has been measured using a force-setpoint of $F_x = F_y = F_z = 15$ N and no torque. The results of the static force and torque measurements are shown in figures 9 and 10, respectively. Figures 11 and 12 show the predicted values using the same settings as the measurement and a semi-analytical model which includes higher harmonics of the magnetic flux density distribution of the magnet array (Jansen, J.W. et al. 2007b) which are not included in the real-time model of the commutation algorithm. The differences between the measured and the predicted values can be explained by the following reasons:

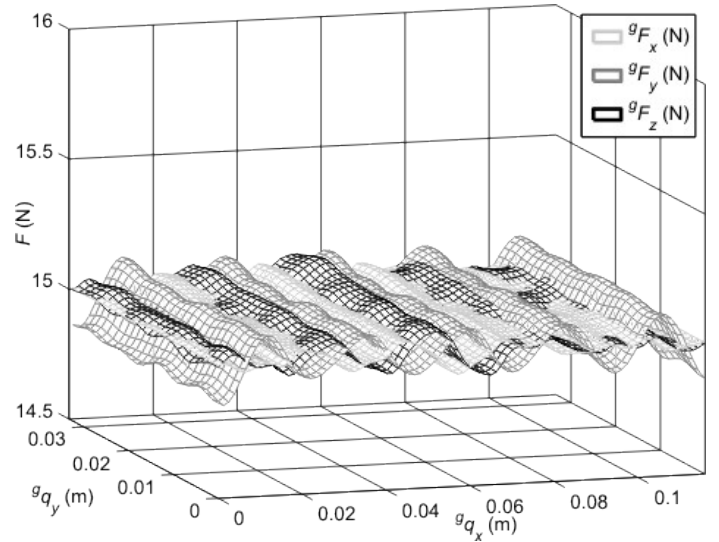


Figure 11. Predicted force components sF_x , sF_y and sF_z of the open-loop commutated HPPA, using a desired wrench vector ${}^s\mathbf{w}_{\text{des}} = [15 \ 15 \ 15 \ 0 \ 0 \ 0]^T$ and a clearance of 1.5 mm

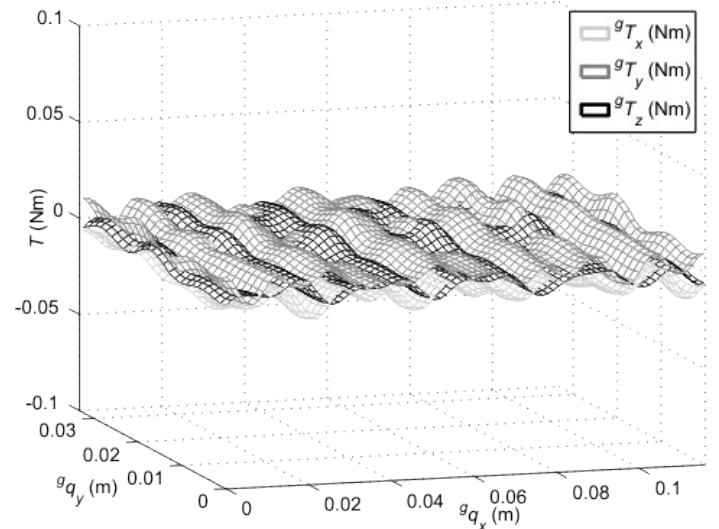


Figure 12. Predicted torque components sT_x , sT_y and sT_z of the open-loop commutated HPPA, using a desired wrench vector ${}^s\mathbf{w}_{\text{des}} = [15 \ 15 \ 15 \ 0 \ 0 \ 0]^T$ and a clearance of 1.5 mm

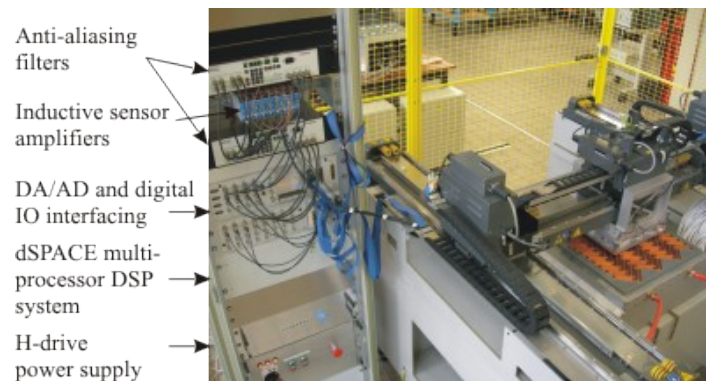


Figure 13. An overview of the planar actuator test-bench

-Misalignment of the translator with respect to the stator coils. Simulations of the HPPA, which is misaligned in the xy -plane, confirm that the ripple of

resulting in a structured dynamical model error which is also shown in the s-plane of Figure 14. In the ideal situation the real-time model equals the ideal model $\Gamma_{1\text{dof}} = \Gamma_{1\text{dof}}^*$ resulting in $F_{\text{dist}} = 0$, $C_1 = 0$ and $C_2 = 1$ which implies that $F = F_{\text{des}}$ leading to a second order differential equation of a mass damping system.

Note that the disturbance force F_{dist} given by equation (6) can be one of the causes of the slightly larger open-loop measured force and torque errors of Figures 9 and 10.

The model error was verified by applying two different commutation matrices $\Gamma^-(q)$ to the real closed loop system. Firstly, a commutation matrix $\Gamma^-(q)$ was used of which the parameters only depended on the (three DOF) position ${}^s q_x$, ${}^s q_y$ and ${}^s q_z$ of the translator and not on the orientation. This results in a commutation error for non-zero angles ${}^s q_\psi$, ${}^s q_\theta$ and ${}^s q_\phi$. Which are the rotations about the x , y and z axis, respectively. Secondly, a commutation matrix $\Gamma^-(q)$ was used which did include the angles ${}^s q_\psi$ and ${}^s q_\theta$ (five DOF). Figure 15 shows the reconstructed normalized frequency response of the angular acceleration towards the angle ${}^s \ddot{q}_\psi \rightarrow {}^s \ddot{q}_\psi$, when applying the two commutation matrices, using closed-loop noise identification of the HPPA. The errors caused by the commutation matrix depending

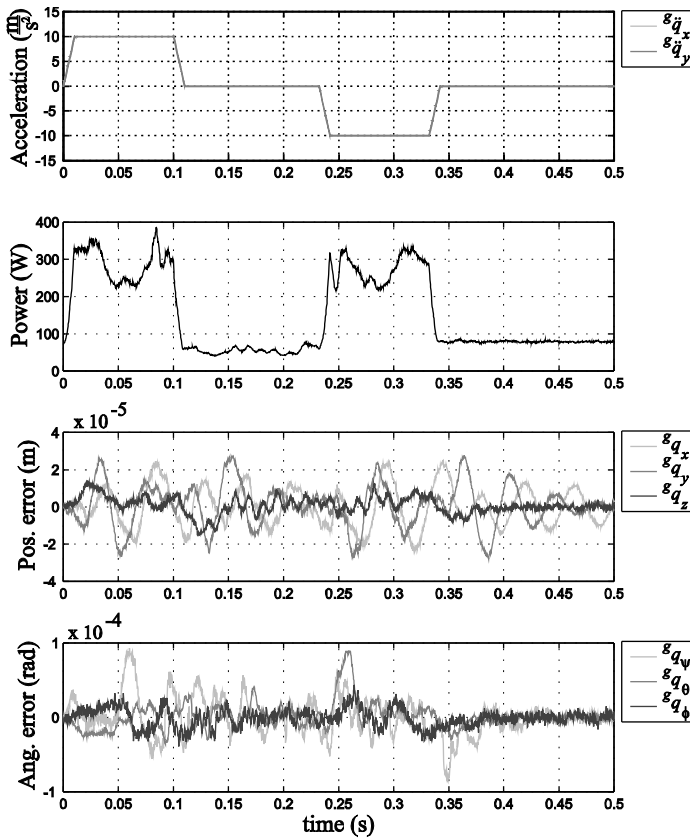


Figure 16. Acceleration profile, estimated power dissipation and the position and angle errors of the translator of the HPPA during movement on trajectory e-e' defined in Figure 4 with a mechanical clearance of 1 mm.

on three DOF clearly result in a resonance peak whereas the five DOF dependent matrix does not result in a resonance peak. This can be explained by looking at the root-locus plot in the s-plane shown in Figure 14. The commutation error causes a shift in the two real poles of the mechanical mass damping system towards a set of badly damped complex poles. Nevertheless, the shift is only minor when a stiff bearing controller is used to stabilize the rotations of the translator. Therefore, when a stiff bearing controller is applied it is possible to use a commutation matrix which parameters do not depend on the angles. This could be useful to reduce the calculation time of the commutation algorithm. However, care should be taken when performing closed loop noise identification of the actuator because generally this should be done using a weak controller which can result in the position dependent resonances of which an example is shown in Figure 15.

The typical long stroke closed-loop performance of the HPPA is shown in Figure 16 which shows the acceleration profile the estimated power dissipation and both the position and the angle tracking errors of the HPPA, when applying trajectory e-e' which is defined in Figure 4 with a maximum speed of 1.4 m/s and a mechanical clearance of 1 mm. Note that the trajectory e-e' uses an acceleration of 10 m/s² in both the ${}^s q_x$ as well as the ${}^s q_y$ direction resulting in an amplitude of the acceleration vector in the xy -plane of approximately 14 m/s². According to Figure 6 this could violate the current amplifier constraints. However, the acceleration vector in the xy -plane of the chosen trajectory is oriented orthogonal to the worst-case direction (indicated in Figure 7) enabling a larger acceleration without violating the constraints.

The six identical normalized feedback controllers (divided by the mass or inertia for the force or the torque controllers, respectively) with a bandwidth of 330 rad/s which have been used during this tracking error experiment are given by

$$C_n(s) = 4.18 \cdot 10^5 \frac{(s+66)^2}{s(s+1320)^2} \quad (2)$$

and six acceleration feedforward controllers have been added. From Figure 16 it can be seen that the measured ${}^s q_x$ and ${}^s q_y$ position errors contain a low frequency oscillation which, most probably, corresponds to a base-frame oscillation of the test-bench which is excited by the large moving mass of the H-drive in the xy -plane. Moreover, the dynamics of the H-drive joints disturb the position measurement of the translator. Furthermore, the anti-aliasing filters which are used to filter the inductive

position sensors cause a large phase delay which limits the feedback control bandwidth. Nevertheless, a tracking error of less than 30 μm and 0.1 mrad has been obtained. Future research will focus on improving the test setup by improving the measurement accuracy and removing the test-bench disturbances.

5 CONCLUSIONS

In this paper several experiments have been performed on a moving-magnet planar actuator topology with integrated magnetic bearing called the Herringbone Pattern Planar Actuator (HPPA). A special commutation strategy called direct wrench-current decoupling has been derived which allows for switching between different active sets of coils without influencing the decoupling of the force and torque components. Due to the switching and the need to decouple both the force and the torque, the resulting current waveforms are non-sinusoidal and each stator coil needs to be controlled individually using a single phase amplifier. To obtain correct trajectories, during the experiments, which do not violate the current amplifier constraints a novel method is presented in this paper to derive the worst-case acceleration specification in the xy -plane, as a function of the current amplifier constraints.

Open-loop (static) force and torque measurements show the correct decoupling of the special commutation algorithm. Therefore, six SISO controllers have been used in the (dynamic) closed-loop experiments. A theory of the structured dynamical model errors has been derived and validated by a measured frequency response. The tracking errors during a demanding trajectory with a maximum acceleration of 14 m/s^2 and a maximum speed of 1.4 m/s are less than 30 μm and less than 0.1 mrad for the position and orientation, respectively. The current performance limitations are caused by the test-bench in which the experiments have been conducted. Future research will focus on improving the test setup by improving the measurement accuracy and removing the test-bench disturbances.

6 REFERENCES

- Jansen, J.W., Lierop, C.M.M. van, Lomonova, E.A., Vandenput, A.J.A. 2007a. Magnetically levitated planar actuator with moving magnets. *IEEE International Electric Machines and Drives Conference (IEMDC'07), Antalya, Turkey*: 272–278.
- Lierop, C.M.M. van, Jansen, J.W., Damen, A.A.H., Bosch, P.P.J. van den 2006. Control of multi-degree-of-freedom planar actuators. *Proceedings of the 2006 IEEE*

International Conference on Control Applications, CCA 2006, Munich, Germany: 2516–2521.

- Lierop, C.M.M. van, Jansen, J.W., Lomonova, E.A., Damen, A.A.H., Vandenput, A.J.A. & Bosch, P.P.J. van den 2007. Commutation of a magnetically levitated planar actuator with moving-magnets. *Proceedings of the 6th international symposium on linear drives for industrial applications, Lille, France*.

- Jansen, J.W., Lierop, C.M.M. van, Lomonova, E.A. & Vandenput, A.J.A. 2007b. Modeling of magnetically levitated planar actuators with moving magnets. *IEEE Transactions on Magnetics* 43(1): 15–25.